

# Selective Molecular–Complex Phase Formation of Syndiotactic Polystyrene with a Styrene Dimer

Nunzia Galdi, Alexandra R. Alburnia, Leone Oliva, and Gaetano Guerra\*

Dipartimento di Chimica, Università di Salerno, I-84084 Fisciano (SA), Italy

Received September 19, 2006; Revised Manuscript Received October 6, 2006

**ABSTRACT:** The possible formation of molecular–complex phases of s-PS with styrene dimers has been investigated by their sorption in amorphous and nanoporous  $\delta$ -form films. X-ray diffraction,  $^{13}\text{C}$  solid state NMR, and FTIR analyses have shown that only 1,3-diphenylbutane (dpb), but not 1,4-diphenylbutane, forms a highly stable molecular–complex with s-PS. Preliminary structural considerations indicate that this s-PS/dpb molecular–complex phase presents an intercalate structure, with host-monomer-unit/guest stoichiometric ratio of 4/1 and with a guest conformation with anti C2–C3 bond. Guest conformational behavior has allowed to discriminate, for the first time by a NMR technique, between guest molecules located in crystalline and amorphous s-PS phases. Presently dpb is the s-PS guest with maximum volume ( $\approx 0.36 \text{ nm}^3$ ) and maximum number of non-hydrogen atoms ( $n = 16$ ).

## Introduction

The complex polymorphic behavior of syndiotactic polystyrene (s-PS) has been extensively studied.<sup>1</sup> In particular, great attention has been devoted to its ability to form molecular–complex crystalline phases with a large variety of low molecular weight substances.<sup>1,2</sup> By suitable removal of the guest molecules from any of these molecular–complex phases it is possible to obtain a nanoporous metastable polymorph of s-PS, the  $\delta$  form, a host phase including centrosymmetric crystalline cavities (of nearly  $120\text{--}160 \text{ \AA}^3$ ) in a molar ratio of 1/4 with respect to the styrene monomeric units.<sup>3</sup> Since this form is able to rapidly and selectively absorb some organic substances from various environments (producing crystalline host–guest molecular–complexes) its employment in the field of molecular sieves for purification of water or gases<sup>4</sup> or as a sensing film for molecular sensors<sup>5</sup> has been proposed.

For most s-PS molecular–complexes, isolated low-molecular-mass compounds are imprisoned as guest into the cavities of the nanoporous host  $\delta$  phase, only producing minor changes to the packing of the polymer helices.<sup>2,3</sup> These s-PS molecular–complexes have been defined as *clathrate* phases and are generally characterized by a guest/monomeric-unit molar ratio 1/4.

Only recently, the occurrence of a different class of s-PS molecular–complexes, defined as *intercalate* rather than *clathrate*, has been established.<sup>6</sup> In fact, for some s-PS molecular–complexes (e.g. with norbornadiene<sup>6a</sup> or 1,3,5-trimethylbenzene<sup>6b</sup> or 1,4-dimethylnaphthalene<sup>6b</sup>) the guest molecules are not isolated into host cavities but contiguous inside layers intercalated with monolayers of enantiomorphous polymer helices. Of course, these intercalate structures present a higher guest content with respect to the clathrate structures and the guest/monomeric-unit molar ratio generally is 1/2 rather than 1/4.

The self-assembling of the polymer host  $\delta$  phase and several active guest molecules into crystalline molecular–complexes can be relevant for several applications. In fact, polymer-based host–guest molecular–complexes not only reduce the guest diffusivity and prevent guest self-aggregation (without recurring to chemical reactions), but also allow to control at molecular level the location and orientation of active guest molecules. On this basis, films presenting s-PS/active-guest molecular–

complex phases have been proposed as advanced materials, mainly for optical applications (e.g., as fluorescent, photoreactive, and chromophoric materials).<sup>7</sup>

However, the formation of molecular–complex phases with s-PS has been limited by the guest size. In fact, until now the guests with maximum volume are *n*-decane<sup>8a</sup> ( $\approx 0.32 \text{ nm}^3$ ) and decahydronaphthalene<sup>6b</sup> ( $\approx 0.26 \text{ nm}^3$ ) while the guests with maximum number of non-hydrogen atoms are anthracene<sup>8b</sup> ( $n = 14$ ) and 1,4-dimethylnaphthalene<sup>6b</sup> ( $n = 12$ ).

Recently some of us reported a route to quantitatively convert styrene into low molecular weight oligomers such as 1,3-diphenylbutane, 1,4-diphenylbutane, 1,3,5-triphenylhexane, and 1,3,6-triphenylhexane.<sup>9</sup> The synthesis proceeds through a poly-insertion process catalyzed by *ansa*-zirconocenes activated by methylaluminoxane, in the presence of hydrogen. The feed composition as well as the kind of *ansa*-zirconocene employed as catalyst determinates the oligomers composition.

In this study we have explored the possible formation of molecular–complex phases of s-PS with styrene dimers. Our analysis has shown that s-PS selectively forms a highly stable intercalate molecular–complex with 1,3-diphenylbutane, which is presently the s-PS guest with maximum volume ( $\approx 0.36 \text{ nm}^3$ ) and maximum number of non-hydrogen atoms ( $n = 16$ ).

## Experimental Part

**Materials. Synthesis of the Dimers.** All manipulations of air-sensitive compounds have been performed through glovebox or Schlenk techniques. The styrene was stirred over  $\text{CaH}_2$  before distillation under reduced pressure. The commercial methylaluminoxane (30% in toluene from Witco) was dried by removing in a vacuum the solvent and the traces of trimethylaluminum and was used as a powder.

For the synthesis of 1,3-diphenylbutane, *rac*- $\text{CH}_2[3\text{-}i\text{-C}_3\text{H}_7\text{-1-Ind}]_2\text{ZrCl}_2$  has been employed, synthesized according to the literature.<sup>10</sup> A 100 mL steel autoclave thermostated at  $65^\circ\text{C}$  was evacuated and then charged with 30 mL of a solution of MAO (1.2 g) and of the zirconocene (15 mg) in styrene. The reactor was feed with  $\text{H}_2$  at the constant pressure of 7 atm and mechanically stirred. After 8 h, the hydrogen was vented off and the reaction mixture was poured into acidified ethanol. By shaking with water and *n*-pentane ( $3\times$ ), the organic phase was separated and recovered. After anhydrication of the solution with  $\text{Na}_2\text{SO}_4$  the pentane was removed under reduced pressure and a yellow oily mixture of

oligomers was recovered. A distillation under reduced pressure afforded pure 1,3-diphenylbutane (bp 105–110 at 1 Torr, yield 5.6 g).

The 1,4-diphenylbutane was obtained in the presence of the catalytic system *rac*-ethylenebis(4,5,6,7-tetrahydroindenyl)zirconium dichloride (purchased from MCAT) activated by methylaluminoxane. The hydrooligomerization was carried out under atmospheric pressure of hydrogen in a 100 mL glass flask. Twenty milliliters of the solution of MAO (0.41 g) and zirconocene (3 mg) in styrene was magnetically stirred for 18 h at 50 °C then poured into acidified ethanol and treated as above-described for 1,3-diphenylbutane. The distillation, under reduced pressure, afforded the 1,4-diphenylbutane, which was further purified by crystallization from ethanol (mp 52–54 °C), yield 9 g.

Syndiotactic polystyrene was supplied by Dow Chemical under the trademark Questra 101.  $^{13}\text{C}$  nuclear magnetic resonance characterization showed that the content of syndiotactic polystyrene triads was over 98%. The weight-average molar mass obtained by gel permeation chromatography (GPC) in trichlorobenzene at 135 °C was found to be  $M_w = 3.2 \times 10^5$  with the polydispersity index,  $M_w/M_n = 3.9$ .

Amorphous films, 80–120  $\mu\text{m}$  thick, have been obtained by melt extrusion.

The  $\delta$  form s-PS films presenting the (010) uniplanar orientation have been obtained by casting from 0.5 wt % chloroform solution at room temperature.

**Characterization Methods.** The guest content was determined by thermogravimetric analysis (TGA) carried out by a Mettler TG50 thermobalance in a flowing nitrogen atmosphere at a heating rate of 10 °C/min.

Wide-angle X-ray diffraction patterns with nickel-filtered Cu K $\alpha$  radiation were obtained, in reflection, with an automatic Bruker diffractometer.

Infrared spectra were obtained at a resolution of 2.0  $\text{cm}^{-1}$  with a Vector 22 Bruker spectrometer equipped with deuterated triglycine sulfate (DTGS) detector and a KBr beam splitter. The frequency scale was internally calibrated to 0.01  $\text{cm}^{-1}$  using a He–Ne laser. A total of 32 scans were signal averaged to reduce the noise.

Differential scanning calorimetry (DSC) measurements were carried out with a DSC 2920 TA Instruments in a flowing nitrogen atmosphere, at a heating rate of 10 °C/min.

$^{13}\text{C}$  NMR measurements were performed on Bruker Avance 300 (75.48 MHz for  $^{13}\text{C}$  Larmor frequency). Solution high-resolution spectra were collected using a pulse length of 7.8  $\mu\text{s}$  (90°) and an acquisition time of 0.7 s with a relaxation delay of 1 s to ensure quantitative analysis. Solid-state spectra were acquired using a CP-MAS pulse sequence with a contact time of 2 ms using a 4 mm sample tube. Pulse length of 90° (8  $\mu\text{s}$ ) and an acquisition time of 0.049 s with a relaxation delay of 3 s were used to ensure quantitative detection. For a typical solid state  $^{13}\text{C}$  NMR spectrum 30K transients were accumulated.

The molecular volume of the guest molecules has been simply evaluated from their molecular mass ( $M$ ) and density ( $\rho$ ):

$$V_{\text{guest}} = M/\rho N_A$$

where  $N_A$  is Avogadro's number ( $6.02 \times 10^{23}$  molecules/mol).

## Results

**X-ray Diffraction.** Sorption of the styrene dimer 1,4-diphenylbutane into s-PS amorphous samples as well as in semicrystalline  $\delta$  form s-PS samples induces crystallization in the  $\gamma$  phase, as occurs for most solute molecules much bigger than the cavity of the  $\delta$  s-PS phase.<sup>1c</sup>

Sorption of the styrene dimer 1,3-diphenylbutane (thereafter dpb) into s-PS amorphous samples, as well as in semicrystalline  $\delta$  form s-PS samples, instead generates a stable molecular–complex crystalline phase.

The X-ray diffraction pattern of an amorphous s-PS film immersed in dpb for 3 days at room temperature has been

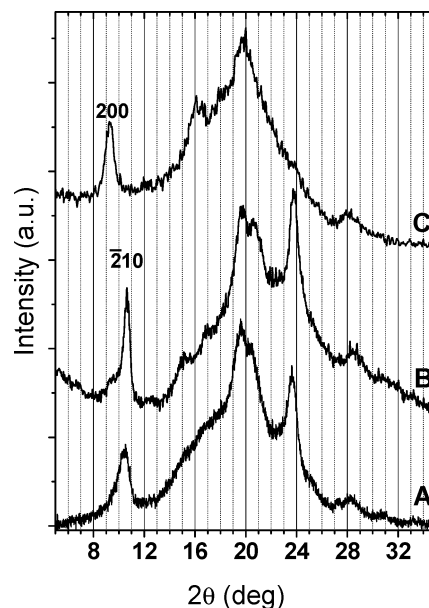


**Figure 1.** X-ray diffraction patterns of amorphous s-PS films: (A) after immersion in dpb for 3 days at room temperature; (B) after annealing of 3 h at 100 °C followed by treatment under vacuum at 70 °C for 6 days; (C) after treatment for 20 min at 130 °C.

reported in Figure 1A. The X-ray diffraction patterns of the same film, after annealing of 3 h at 100 °C followed by treatment under vacuum at 70 °C for 6 days, and after treatment for 20 min at 130 °C are also reported in Figure 1, parts B and C, respectively.

The dpb content of the three samples of Figure 1, as evaluated by thermogravimetric analysis is 34%, 18%, and 30%, respectively.

The pattern of Figure 1A clearly indicates the occurrence of a solvent-induced crystallization while the pattern of Figure 1B shows that bigger and more perfect crystallites are formed as a consequence of annealing at 100 °C. In particular, the intense and narrow peak observed for  $2\theta_{\text{Cu K}\alpha} = 10.6^\circ$  (corresponding to a Bragg distance  $d = 0.83$  nm) in Figure 1B, suggests the occurrence of uniplanar orientation analogous to the (210) one (i.e., such as the crystallographic planes (210) are nearly parallel to the film plane)<sup>11</sup> which have been observed for s-PS molecular–complex phases with 1,4-dimethylnaphthalene and with *o*-xylene, when these guests are absorbed in amorphous films.<sup>11</sup> This hypothesis has been confirmed by X-ray diffraction patterns taken with beam parallel and perpendicular to the film plane and collected on a photographic cylindrical camera, which are analogous to those shown in Figure 3, parts A and B, of ref 11, respectively, hence indicating the occurrence of analogous uniplanar crystalline phase orientations.

The X-ray diffraction pattern of Figure 1C clearly indicates the presence of a  $\gamma$  phase with a (200) uniplanar orientation, as usually observed as a consequence of annealing in the temperature range 120–170 °C of molecular–complex phases with uniplanar (210) orientation.<sup>11</sup>

Additional information relative to this molecular–complex can be easily achieved by its formation by dpb sorption in films presenting oriented  $\delta$  phases. For instance, the X-ray diffraction pattern of a  $\delta$ -form s-PS film presenting uniplanar (010) orientation,<sup>12</sup> after immersion in dpb for 7 days at 55 °C (then treated under vacuum for 3 days at 70 °C), whose dpb content is close to 20%, has been reported in Figure 2. The pattern clearly shows peaks with Miller indexes (010), (020), and (030), corresponding to three orders of a periodicity of 1.4 nm. As

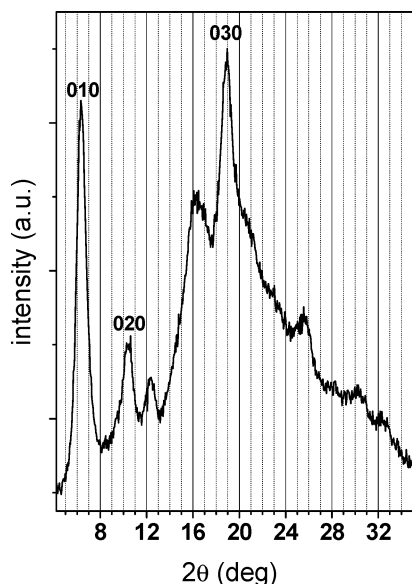


**Figure 2.** X-ray diffraction pattern of an s-PS film with (010) orientation of the  $\delta$ -phase, after immersion in dpb for 7 days at 55 °C, followed by treatment under vacuum at 70 °C for 3 days.

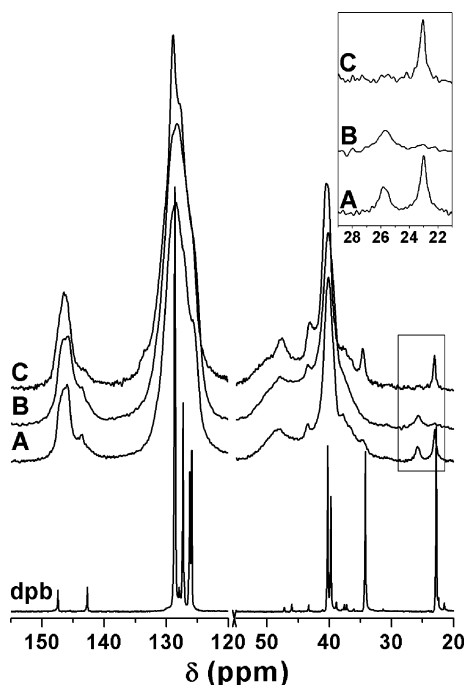


**Figure 3.**  $^{13}\text{C}$  solid-state NMR spectra of amorphous s-PS films: (A) after immersion in dpb for 3 days at room temperature; (B) after annealing of 3 h at 100 °C followed by treatment under vacuum at 70 °C for 6 days; (C) after treatment for 20 min at 130 °C, presenting the X-ray diffraction patterns shown in Figure 1A–C. The solution  $^{13}\text{C}$  spectrum ( $\text{CDCl}_3$ ) of the dpb is shown in the bottom of the figure.

discussed in detail in Figure 4 of ref 6b, this large periodicity clearly suggests the presence of an intercalate rather than a clathrate molecular–complex phase.

**NMR Analysis.**  $^{13}\text{C}$  solid-state NMR spectra of the three film samples of Figure 1A–C are reported as traces A–C in Figure 3. For comparison purpose, the solution  $^{13}\text{C}$  spectrum ( $\text{CDCl}_3$ ) of the dpb with aliphatic resonances at  $\delta$  22.7 (C-4), 34.2 (C-1), 39.7 (C-3) and 40.2 (C-2) and aromatic resonances between  $\delta$  125.8 and 147.4, is also shown in the bottom of Figure 3.

As for the solid state spectra, beside the main signals of s-PS one can observe some less intense resonances assignable to dpb and particularly informative is the methyl region (inset on the

right of Figure 3). In particular, for the molecular–complex film of lower crystallinity and higher dpb content ( $\approx 30$  wt %, Figure 3A) two peaks are observed: one at a chemical shift value very close to that observed in the solution spectrum ( $\delta$  22.7 ppm) and a second one situated downfield ( $\delta$  25.7 ppm). The upfield peak is largely prevalent for the  $\gamma$ -form film (Figure 3C), containing dpb molecules only in the amorphous phase, while the downfield peak is largely prevalent (Figure 3B) for the molecular–complex film of higher crystallinity and lower dpb content ( $\approx 18$  wt %).

These data can be easily rationalized by assuming that the upfield peak is due to dpb molecules dissolved in the amorphous phase, having a conformational freedom similar to that one occurring in solution, while the downfield peak is due to dpb molecules being guest of the s-PS/dpb molecular–complex phase.

The observed downfield shift suggests that the dpb guest molecules assume a conformation with a reduced number of C–C  $\gamma$ -gauche interactions for the methyl group, while equilibrium between several conformers is expected to occur for dpb molecules in the s-PS amorphous phase. In particular, the NMR analysis suggests that the dpb guest conformer presents an anti C2–C3 bond. It is however worth adding that the downfield shift of the methyl resonance could in principle be due to intermolecular packing interactions in the crystalline phase, as suggested for the crystalline phase of a styrene trimer.<sup>13</sup>

In this framework we can assume that, for the desiccated and annealed film of Figure 3B containing 18 wt % of dpb, most solute molecules are guests of the molecular complex-phase. For the same film, the degree of crystallinity, as evaluated by following the FTIR method described in ref 14, is about 40 wt %. This indicates that the s-PS/dpb intercalate molecular–complex phase presents host-monomer-unit/guest stoichiometric ratio close to 4/1, i.e., a stoichiometry completely different from that one generally observed for s-PS intercalate structures (2/1)<sup>6a,b</sup> and equal to that one generally observed for s-PS clathrate structures.<sup>2</sup> This stoichiometry, unprecedented for s-PS intercalate structures, could be due to the unusually large bulkiness of the dimer guest.

It is worth noting that the evaluation of the peak intensities in the methyl region of the  $^{13}\text{C}$  solid-state NMR spectra (inset of Figure 3) allows a easy quantification of solute molecules simply absorbed in the amorphous phase and those present as guest of the molecular–complex phase. In this respect, it is worth adding that quantitative evaluations of the guest amount in both s-PS phases have been already effected, but only by Fourier transform infrared measurements,<sup>15</sup> for other guest molecules (chlorinated), which present different conformational equilibria in the amorphous and crystalline phases.

**Fourier Transform Infrared Spectra.** FTIR spectra in the wavenumber ranges 1220–1140  $\text{cm}^{-1}$  and 600–480  $\text{cm}^{-1}$  of the three film samples of Figure 1A–C are reported as traces A–C in Figure 4. For the sake of comparison, the FTIR spectrum of a nanoporous  $\delta$ -form film is also shown in Figure 4, as curve D.

These spectra give additional evidences of formation of an s-PS/dpb molecular–complex phase. In particular, the intensity of the host helical s-PS peak at 1167  $\text{cm}^{-1}$  is for the amorphous sample treated by dpb (curves A and B in Figure 4) definitely larger than for the  $\gamma$  and  $\delta$  form films (curves C and D in Figure 4), as typical of s-PS molecular–complex phases.<sup>16</sup>

Moreover, the dpb peak (enlarged in the right part of Figure 4), which is located at 589  $\text{cm}^{-1}$  both for molecules in diluted solutions of noninteracting solvent (dotted line) as well as for



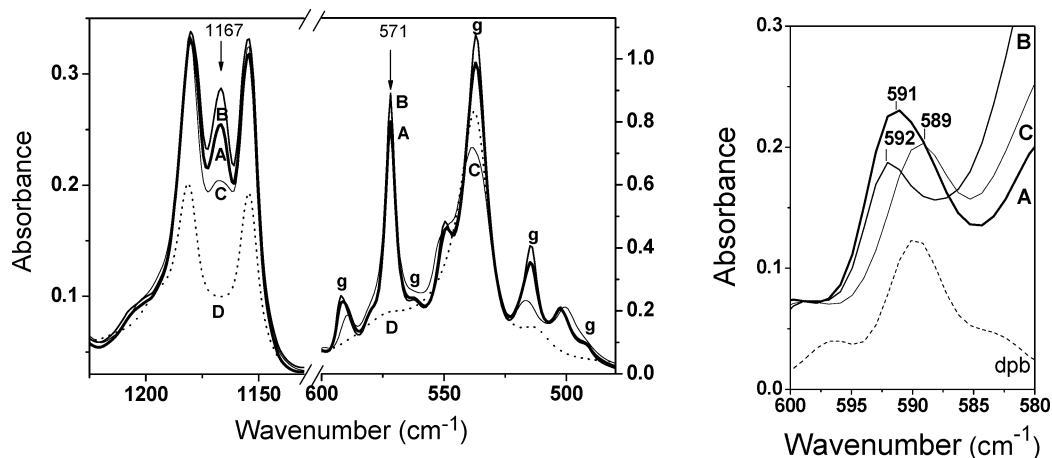


**Figure 4.** FTIR spectra in the wavenumber ranges 1220–1140  $\text{cm}^{-1}$  and 600–480  $\text{cm}^{-1}$  of amorphous s-PS films: (A) after immersion in dpb for 3 days at room temperature; (B) after annealing of 3 h at 100  $^{\circ}\text{C}$  followed by treatment under vacuum at 70  $^{\circ}\text{C}$  for 6 days; (C) after treatment for 20 min at 130  $^{\circ}\text{C}$ , presenting the X-ray diffraction patterns shown in Figure 1A–C, respectively. The FTIR spectrum of the host  $\delta$ -form film is shown as curve D. Guest peaks have been specifically labeled by a g and the guest peak at 589  $\text{cm}^{-1}$  has been enlarged in the right part of the figure.

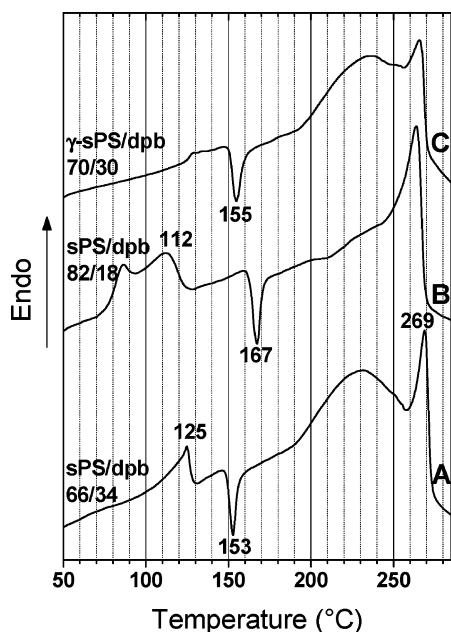


**Figure 5.** DSC scans of amorphous s-PS films: (A) after immersion in dpb for 3 days at room temperature; (B) after annealing of 3 h at 100  $^{\circ}\text{C}$  followed by treatment under vacuum at 70  $^{\circ}\text{C}$  for 6 days; (C) after treatment for 20 min at 130  $^{\circ}\text{C}$ , presenting the X-ray diffraction patterns shown in Figure 1A–C. The initial dpb content is indicated close to the curves.

solute molecules in the amorphous phase of the  $\gamma$ -phase film (curve C), is shifted at 591 and 592  $\text{cm}^{-1}$  for guest molecules of molecular–complex phases (curves A and B). This peak shift to lower frequency clearly indicates the occurrence of host–guest attractive interactions between s-PS and the styrene dimer. Analogous low-frequency shifts have been observed for guest peaks of molecular–complex phases of s-PS with chloroform,<sup>14b</sup> 1,2-dichloroethane,<sup>17</sup> and *n*-alkanes.<sup>18</sup>

**Differential Scanning Calorimetry.** DSC scans of the three film samples of Figure 1A–C are reported as traces A–C in Figure 5.

The DSC scan of the  $\gamma$ -form film of Figure 5C is typical of a  $\gamma$ -form sample in the presence of a highly boiling solvent.<sup>1c</sup> In fact, beside a minor endothermic peak at nearly 130  $^{\circ}\text{C}$ , produced as a consequence of the annealing procedure used, a narrow exothermic peak at 155  $^{\circ}\text{C}$ , corresponding to the  $\gamma \rightarrow$

$\beta$  transition (as generally observed for  $\gamma$ -form samples when heated in the presence of highly boiling solvents),<sup>1c</sup> a broad endothermic peak in the temperature range 190–260  $^{\circ}\text{C}$ , corresponding to the evaporation of the highly boiling dpb molecules, and a narrow endothermic peak close to 270  $^{\circ}\text{C}$ , corresponding to the melting of the s-PS  $\beta$ -phase, are observed.

The DSC scan of the molecular–complex film of Figure 5A shows a well-defined endothermic peak at 125  $^{\circ}\text{C}$ , which (on the basis of X-ray diffraction spectra like those of Figure 1) is associated with the transition from the molecular–complex phase toward the  $\gamma$ -phase, also leading to a confinement of the dpb molecules in the amorphous phase. After this phase transition, the film behaves as the  $\gamma$ -phase film of Figure 5C: a narrow exothermic peak at 153  $^{\circ}\text{C}$ , corresponding to the  $\gamma \rightarrow \beta$  transition, the broad and intense endothermic peak corresponding to the evaporation of the highly boiling dpb molecules and a narrow endothermic peak corresponding to the melting of the s-PS  $\beta$ -phase.

The DSC scan of the annealed molecular–complex film of Figure 5B is rather similar to that one of Figure 5A. The endotherm corresponding to the molecular–complex  $\rightarrow \gamma$  transition is more intense due to the higher crystallinity (cf. Figure 1, parts A and B) and presents two peaks, due to the annealing temperatures used (70 and 100  $^{\circ}\text{C}$ ). Moreover, the dpb broad evaporation endotherm is much less pronounced, due to its lower dpb content. It is worth adding that, by reducing the amount of dpb from 34 to 18 wt %, the temperature of the  $\gamma \rightarrow \beta$  transition increases from 153  $^{\circ}\text{C}$  up to 167  $^{\circ}\text{C}$ , in good qualitative agreement with the results reported in Figures 4 and 5 of ref 1c for  $\gamma$ -form films with 1-chlorotetradecane.

It is also worth noting that for the s-PS/dpb molecular–complex phase the transition toward the  $\gamma$ -phase is well apparent and not hidden by the guest evaporation, as occurs for most s-PS molecular–complexes.<sup>1a,b,6c,19</sup> In fact, in the present case the guest molecules rejected from the crystalline phase remain in the amorphous phase and evaporate only for temperatures above 190  $^{\circ}\text{C}$ .

## Conclusions

The possible formation of molecular–complex phases of s-PS with styrene dimers has been explored by their sorption in amorphous and nanoporous  $\delta$ -form films. X-ray diffraction,<sup>13</sup> solid state NMR and FTIR analyses have shown that the styrene

dimer, 1,3-diphenylbutane (dpb), forms a highly stable molecular–complex with s-PS, both starting from amorphous samples and from  $\delta$ -form samples, whose crystallinity can be improved by annealing. On the other hand, a different styrene dimer, 1,4-diphenylbutane, does not form a molecular–complex phase with s-PS at least in the considered experimental conditions.

The large value of the Bragg distance relative to the (010) plane suggests that the s-PS/dpb molecular–complex phase is an intercalate rather than a clathrate phase.<sup>6</sup> This molecular–complex phase, when obtained by guest-treatment of amorphous s-PS films, presents an uniplanar orientation analogous to the (210) orientation observed for treatments of s-PS amorphous films with 1,4-dimethylnaphthalene or *o*-xylene.<sup>11</sup>

The methyl region of <sup>13</sup>C solid-state NMR spectra shows, beside an upfield peak due to dpb molecules dissolved in the polymer amorphous phase, a well separated downfield peak due to dpb molecules being guest of the crystalline molecular–complex phase. This kind of analysis on different s-PS films shows that, as a consequence of vacuum treatments and annealing up to 100 °C, most dpb molecules remain as guest of the crystalline molecular–complex phase, while the dpb content in the amorphous phase can become negligible. It is worth noting that for the first time a NMR technique has allowed to quantitatively discriminate between solute molecules simply absorbed in the amorphous s-PS phase and those present as guest of the molecular–complex phase.

The observed downfield shift of its methyl resonance suggests that the dpb guest conformer has anti C2–C3 bond. Moreover, thermogravimetric measurements of guest content ( $\approx 18$  wt %) and FTIR evaluations of the degree of crystallinity ( $\approx 40$  wt %) of a film presenting only the downfield methyl peak (and hence having guest molecules essentially only in the crystalline phase) suggest a stoichiometric ratio host-monomeric-units/guest close to 4/1.

FTIR spectra give additional evidences of formation of an s-PS/dpb molecular–complex phase. In particular, a shift to lower frequency of the guest peak at 589 cm<sup>-1</sup> clearly indicates the occurrence of host–guest attractive interactions between s-PS and the styrene dimer.

Endothermic and exothermic peaks of DSC scans of samples presenting the s-PS/dpb molecular–complex phase have been rationalized on the basis of X-ray diffraction measurements on thermally treated samples and on the basis of previous knowledge on s-PS thermal behavior in the presence of highly boiling solvents.<sup>1c</sup> The transition from the s-PS/dpb molecular–complex phase toward the  $\gamma$ -phase can occur at temperature as high as 125 °C and produces rejection of the guest molecules from the crystalline phase toward the amorphous phase. The removal of the dpb molecules from the amorphous phase occurs only in the temperature range 190–260 °C, i.e., well above the  $\gamma \rightarrow \beta$  phase transition.

Presently dpb is the s-PS guest with maximum volume ( $\approx 0.36$  nm<sup>3</sup>) and maximum number of non-hydrogen atoms ( $n = 16$ ). Our preliminary structural considerations also suggest that this would be the first s-PS intercalate with a host-monomer-unit/guest molar ratio 4/1 (as generally observed for s-PS clathrates) rather than 2/1. X-ray diffraction studies on uniaxially oriented films containing the s-PS/dpb molecular–complex phase are in progress, aiming to define its crystalline structure.

The selective and stable self-assembling of s-PS only with a particular styrene dimer could be in principle exploited to separate styrene dimers. Additional studies, aiming to establish if selective and stable self-assembling of s-PS could occur also with other styrene oligomers, are also in progress.

**Acknowledgment.** Financial support of the “Ministero dell’Istruzione, dell’Università e della Ricerca” (PRIN2004); and of “Regione Campania” (Legge 5) is gratefully acknowledged. We thank Prof. Vittorio Petraccone of University of Naples for useful discussions and Dr Patrizia Oliva of the University of Salerno for assistance in the use of 300 MHz NMR spectrometer.

## References and Notes

- (1) (a) Guerra, G.; Vitagliano, M. V.; De Rosa, C.; Petraccone, V.; Corradini, P. *Macromolecules* **1990**, *23*, 1539–1544. (b) Chatani, Y.; Shimane, Y.; Inoue, Y.; Inagaki, T.; Ishioka, T.; Iijitsu, T.; Yukimori, T. *Polymer* **1992**, *33*, 488–492. (c) Rizzo, P.; Albulia, A. R.; Guerra, G. *Polymer* **2005**, *46*, 9549–9554.
- (2) (a) Immirzi, A.; de Candia, F.; Iannelli, P.; Zambelli, A.; Vittoria, V. *Makromol. Chem., Rapid Commun.* **1988**, *9*, 761–764. (b) Chatani, Y.; Shimane, Y.; Inagaki, T.; Iijitsu, T.; Yukimori, T.; Shikuma, H. *Polymer* **1993**, *34*, 1620–1624. (c) Chatani, Y.; Inagaki, T.; Shimane, Y.; Shikuma, H. *Polymer* **1993**, *34*, 4841–4845. (d) Moyses, S.; Sonntag, P.; Spells, S. J.; Laveix, O. *Polymer* **1998**, *39*, 3537–3544. (e) De Rosa, C.; Rizzo, P.; Ruiz de Ballesteros, O.; Petraccone, V.; Guerra, G. *Polymer* **1999**, *40*, 2103–2110. (f) Tarallo, O.; Petraccone, V. *Macromol. Chem. Phys.* **2004**, *205*, 1351–1360. (g) Tarallo, O.; Petraccone, V. *Macromol. Chem. Phys.* **2005**, *206*, 672–679.
- (3) (a) De Rosa, C.; Guerra, G.; Petraccone, V.; Pirozzi, B. *Macromolecules* **1997**, *30*, 4147–4152. (b) Reverchon, E.; Guerra, G.; Venditto, V. *J. Appl. Polym. Sci.* **1999**, *74*, 2077–2082. (c) Milano, G.; Venditto, V.; Guerra, G.; Cavallo, L.; Ciambelli, P.; Sannino, D. *Chem. Mater.* **2001**, *13*, 1506–1511. (d) Amutharani, D.; Yamamoto, Y.; Saito, A.; Sivakumar, M.; Tsujita, Y.; Yoshimizu, H.; Kinoshita, T. *J. Polym. Sci., Part B: Polym. Phys.* **2002**, *40*, 530–536. (e) Yoshioka, A.; Tashiro, K. *Macromolecules* **2003**, *36*, 3593–3600. (f) Tamai, Y.; Fukuda, M. *Polymer* **2003**, *44*, 3279–3289. (g) Ma, W.; Yu, J.; He, J. *Macromolecules* **2005**, *38*, 4755–4760.
- (4) (a) Manfredi, C.; Del Nobile, M. A.; Mensitieri, G.; Guerra, G.; Rapacciuolo, M. *J. Polym. Sci., Polym. Phys. Ed.* **1997**, *35*, 133–140. (b) Guerra, G.; Milano, G.; Venditto, V.; Musto, P.; De Rosa, C.; Cavallo, L. *Chem. Mater.* **2000**, *12*, 363–368. (c) Sivakumar, M.; Yamamoto, Y.; Amutharani, D.; Tsujita, Y.; Yoshimizu, H.; Kinoshita, T. *Macromol. Rapid Commun.* **2002**, *23*, 77–79. (d) Yamamoto, Y.; Kishi, M.; Amutharani, D.; Sivakumar, M.; Tsujita, Y.; Yoshimizu, H. *Polym. J.* **2003**, *35*, 465–469. (e) Daniel, C.; Alfano, D.; Venditto, V.; Cardea, S.; Reverchon, E.; Larobina, D.; Mensitieri, G.; Guerra, G. *Adv. Mater.* **2005**, *17*, 1515–1518. (f) Mahesh, K. P. O.; Tsujita, Y.; Yoshimizu, H.; Okamoto, S.; Mohan, D. *J. Polym. Sci., Part B: Polym. Phys.* **2005**, *43*, 2380–2387. (g) Venditto, V.; De Girolamo Del Mauro, A.; Mensitieri, G.; Milano, G.; Musto, P.; Rizzo, P.; Guerra, G. *Chem. Mater.* **2006**, *18*, 2205–2210. (h) Malik, S.; Roizard, D.; Guenet, J. M. *Macromolecules* **2006**, *39*, 5957–5959.
- (5) (a) Mensitieri, G.; Venditto, V.; Guerra, G. *Sens. Actuators B* **2003**, *92*, 255–261. (b) Giordano, M.; Russo, M.; Cusano, A.; Cutolo, A.; Mensitieri, G.; Nicolais, L. *Appl. Phys. Lett.* **2004**, *85*, 5349–5351. (c) Giordano, M.; Russo, M.; Cusano, A.; Mensitieri, G.; Guerra, G. *Sensors Actuators B* **2005**, *109*, 177–184. (d) Cusano, A.; Pilla, P.; Contessa, L.; Iadicicco, A.; Campopiano, S.; Cutolo, A.; Giordano, M.; Guerra, G. *Appl. Phys. Lett.* **2005**, *87*, 234105/1–234105/3.
- (6) (a) Petraccone, V.; Tarallo, O.; Venditto, V.; Guerra, G. *Macromolecules* **2005**, *38*, 6965–6971. (b) Tarallo, O.; Petraccone, V.; Venditto, V.; Guerra, G. *Polymer* **2006**, *47*, 2402–2410. (c) Malik, S.; Rochas, C.; Guenet, J. M. *Macromolecules* **2006**, *39*, 1000–1007.
- (7) (a) Venditto, V.; Milano, G.; De Girolamo Del Mauro, A.; Guerra, G.; Mochizuki, J.; Itagaki, H. *Macromolecules* **2005**, *38*, 3696–3702. (b) Stegmaier, P.; De Girolamo Del Mauro, A.; Venditto, V.; Guerra, G. *Adv. Mater.* **2005**, *17*, 1166–1168. (c) Uda, Y.; Kaneko, F.; Tanigaki, N.; Kawaguchi, T. *Adv. Mater.* **2005**, *17*, 1846–1850.
- (8) (a) Uda, Y.; Kaneko, F.; Kawaguchi, T. *Macromol. Rapid Commun.* **2004**, *25*, 1900–1904. (b) Tsujita, Y.; Yoshimizu, H.; Okamoto, S. *J. Mol. Struct.* **2005**, *739*, 3–12.
- (9) (a) Izzo, L.; Napoli, M. G.; Oliva, L. *Macromolecules* **2003**, *36*, 9340–9345. (b) Galdi, N.; Della Monica, C.; Spinella, A.; Oliva, L. *J. Mol. Catal. A: Chem.* **2006**, *243*, 106–110.
- (10) Balboni, D.; Moscardi, G.; Baruzzi, G.; Braga, V.; Camurati, I.; Piemontesi, F.; Resconi, L.; Nifant'ev, I. E.; Venditto, V.; Antinucci, S. *Macromol. Chem. Phys.* **2001**, *202*, 2010–2028.
- (11) Rizzo, P.; Spatola, A.; De Girolamo Del Mauro, A.; Guerra, G. *Macromolecules* **2005**, *38*, 10089–10094.

- (12) Rizzo, P.; Lamberti, M.; Albunia, A. R.; Ruiz de Ballesteros, O.; Guerra, G. *Macromolecules* **2002**, *35*, 5854–5860.
- (13) Gomez, M. A.; Jasse, B.; Cozine, M. H.; Tonelli, A. E. *J. Am. Chem. Soc.* **1990**, *112*, 5881–5882.
- (14) (a) Albunia, A. R.; Musto, P.; Guerra, G. *Polymer* **2006**, *47*, 234–242. (b) Musto, P.; Mensitieri, G.; Cotugno, S.; Guerra, G.; Venditto, V. *Macromolecules* **2002**, *35*, 2296–2304.
- (15) (a) Guerra, G.; Manfredi, C.; Musto, P.; Tavone, S. *Macromolecules* **1998**, *31*, 1329–1334. (b) Musto, P.; Manzari, M.; Guerra, G. *Macromolecules* **1999**, *32*, 2770–2776. (c) Musto, P.; Manzari, M.; Guerra, G. *Macromolecules* **2000**, *33*, 143–149.
- (16) (a) Daniel, C.; Guerra, G.; Musto, P. *Macromolecules* **2002**, *35*, 2243–2251. (b) Gowd, E. B.; Nair, S. S.; Ramesh, C.; Tashiro, K. *Macromolecules* **2003**, *36*, 7388–7397.
- (17) (a) Daniel, C.; Alfano, D.; Guerra, G.; Musto, P. *Macromolecules* **2003**, *36*, 5742–5750. (b) Musto, P.; Rizzo, P.; Guerra, G. *Macromolecules* **2005**, *38*, 6079–6089.
- (18) Uda, Y.; Kaneko, F.; Kawaguchi, T. *Macromolecules* **2005**, *38*, 3320–3326.
- (19) (a) Wang, Y. K.; Savage, J. D.; Yang, D.; Hsu, S. L. *Macromolecules* **1992**, *25*, 3659–3666. (b) Manfredi, C.; De Rosa, C.; Guerra, G.; Rapacciuolo, M.; Auriemma, F.; Corradini, P. *Macromol. Chem. Phys.* **1995**, *196*, 2795–2808. (c) de Candia, F.; Guadagno, L.; Vittoria, V. *J. Macromol. Sci., Phys.* **1995**, *B34*, 95–103. (d) Rastogi, S.; Goossens, J. G. P.; Lemstra, P. J. *Macromolecules* **1998**, *31*, 2983–2998. (e) De Rudder, J.; Berghmans, H.; Arnauts, J. *Polymer* **1999**, *40*, 5919–5928.

MA062169O